Molecular Orbital Studies of Hydrogen Bonds. IX. Electron Distribution Analysis

Shin-ichi Yamabe and Keiji Morokuma*

Contribution from the Department of Chemistry, University of Rochester, Rochester, New York 14627. *Received December 7, 1974*

Abstract: The change of electron distribution due to hydrogen bond formation is studied with ab initio techniques. The method to analyze the electron distribution systematically is presented in line with the energy decomposition scheme previously proposed. Three linear hydrogen bonded systems are studied: water dimer, formaldehyde–water, and cyclopropenone–water. The polarization interaction is found to cause a large change in the distribution in the intermolecular region as well as in the intramolecular region. The change of the dipole moment upon water dimer formation is also investigated within the same scheme.

I. Introduction

Since the first ab initio LCAO-SCF-MO calculation for the water dimer was reported,[1] many ab initio studies on hydrogen bonded (H bonded) systems have been carried out and have been shown to be quite reliable in predicting the H bond energy and the relative orientation of component molecules in the complex.[2] In order to explore the origin of H bonding we proposed an energy decomposition scheme in which the H bond energy (E_H) is partitioned into four components, i.e., the electrostatic energy (E_{es}), the exchange repulsion energy (E_{ex}), the polarization energy (E_{pl}), and the charge transfer or delocalization energy (E_{ct}).[3] Their characteristic roles in E_H were examined in detail for $H_2O\cdots H_2O$ and $H_2CO\cdots H_2O$ systems. Recently this scheme has been extended to H bond systems in excited states by the use of the electron-hole-potential (EHP) method.[4]

H bond formation causes electron charge redistribution as well as energy stabilization in the entire system. In view of the usefulness of the energy decomposition analysis, we feel that the electron distribution analysis will provide us an additional and complementary insight to the origin of the H bond. While the energy decomposition analysis focuses on the energy change for the entire system, the electron distribution analysis will emphasize *what part* of the interacting system undergoes a large redistribution of the electron density.

In section II, the method of electron density analysis is introduced. Section III presents the basis sets and geometries. Section IV presents the result of electron distribution and dipole moment analyses for $(H_2O)_2$, and section V gives the result of electron density analysis for H_2CO–H_2O and discusses the similarity and difference between the two systems. Section VI deals with cyclopropenone and discusses its monomer electronic structure, the geometry optimization for a H bond complex with a water molecule, and the electron distribution analysis for the complex in comparison with the H_2CO–H_2O complex. Section VII is a brief conclusion.

II. Method of Electron Distribution Analysis

The method of the electron distribution analysis is an extension of the method used previously in the energy decomposition analysis.[3] Here we present the former briefly in connection with the latter.

(i) The Hartree–Fock wave functions for two individual molecules, A and B, at infinite separation, $\mathbf{A}\Psi_A^0$ and $\mathbf{A}\Psi_B^0$. The energy E_0 is the sum of the energy of the individual molecules. **A** is the antisymmetrizer of the electrons. When the two molecules approach each other, the following wave functions can be defined, assuming the monomer geometries are not changed.

(ii) The Hartree product Φ_1 of the wave functions determined in (i).

$$\Phi_1 = \mathbf{A}\Psi_A^0 \cdot \mathbf{A}\Psi_B^0 \tag{1}$$

The energy difference between E_0 and E_1 is the electrostatic energy E_{es} (>0 for stabilization)

$$E_{es} = E_0 - E_1 \tag{2}$$

The electron density, i.e., the probability of finding an electron at a position r_1 for the wave function Φ_1, is defined as

$$\rho_1(1|1) = \int |\mathbf{A}\Psi_A^0(1,\ldots,m)|^2 d\sigma_1 d\tau_2 \ldots d\tau_m + \int |\mathbf{A}\Psi_B^0(1,\ldots,n)|^2 d\sigma_1 d\tau_2 \ldots d\tau_n \tag{3}$$

where m and n are the number of electrons in A and B, respectively. The integration is to be carried out for all the coordinates except for the space coordinate r_1 of the electron 1. For single determinant wave functions such as the Hartree–Fock wave functions for $A\Psi_A^0$ and $A\Psi_B^0$, eq 3 can be rewritten as

$$\rho_1(1|1) = 2\sum_i^{occ} |A_i^0(1)|^2 + 2\sum_k^{occ} |B_k^0(1)|^2 \tag{4}$$

where A_i^0 and B_k^0 are the Hartree–Fock SCF-MO's for the system A and B, respectively.

(iii) The Hartree product Φ_2 of the wave functions for each molecule determined in the presence of the other molecule. Φ_2 is obtained by the SCF procedure neglecting the differential overlap between A and B.

$$\Phi_2 = \mathbf{A}\Psi_A \cdot \mathbf{A}\Psi_B \tag{5}$$

The difference $E_1 - E_2$ is the energy change due to the polarization of one molecule by the other and vice versa.

$$E_{pl} = E_1 - E_2 \tag{6}$$

Equation 3, when $\mathbf{A}\Psi_A$ and $\mathbf{A}\Psi_B$ are used instead of $\mathbf{A}\Psi_A^0$ and $\mathbf{A}\Psi_B^0$, defines the electron density $\rho_2(1|1)$ associated with Φ_2. The difference between ρ_2 and ρ_1 is the density change $\rho_{pl}(1|1)$

$$\rho_{pl}(1|1) = \rho_2(1|1) - \rho_1(1|1) \tag{7}$$

due to the polarization of the electron density of A by the existence of B and vice versa.

(iv) The Hartree–Fock (antisymmetrized) product Φ_3 of two molecular wave functions.

$$\Phi_3 = \mathbf{A}(\Psi_A^0 \Psi_B^0) \tag{8}$$

The energy difference between E_3 and E_1 is the exchange repulsion energy between the two molecules.

$$E_{ex} = E_1 - E_3 \tag{9}$$

Correspondingly, the electron density is defined as

$$\rho_3(1|1) = \int |\Phi_3(1, \ldots, N)|^2 d\sigma_1 d\tau_2 \ldots d\tau_N \tag{10}$$

where $N = n + m$ is the total number of electrons in the complex. The difference between ρ_3 and ρ_1 is the electron density change ρ_{ex} due to the exchange effect

$$\rho_{ex}(1|1) = \rho_3(1|1) - \rho_1(1|1) \tag{11}$$

The requirement of the Pauli principle causes this density depletion from the overlapping region.

Even though E_3 and ρ_3 can be expressed in terms of MO's of isolated molecules and their overlap integrals, the simplest practical way to calculate them is to Schmidt-orthogonalize MO's of the isolated molecules and use the standard expression for energy and density.

(v) The usual SCF wave function Φ_4 for the entire system.

$$\phi_4 = \mathbf{A}(\psi_A \psi_B) \tag{12}$$

The difference between E_0 and E_4 is the hydrogen bond energy E_H (>0 for stabilization) and includes the charge transfer energy E_{ct} and the coupling term E_{cp} as well as E_{es}, E_{pl}, and E_{ex}.

$$E_H = E_0 - E_4 = E_{es} + E_{pl} + E_{ex} + E_{ct} + E_{cp} \tag{13}$$

From eq 2, 6, 9, and 13 one obtains

$$E_{ct} + E_{cp} = E_2 + E_3 - E_1 - E_4 \tag{14}$$

Since E_{ct} and E_{cp} cannot be separated in the present analysis,[5] and since E_{cp}, the coupling between various energy components, is expected to be small, $E_{ct} + E_{cp}$ is, henceforth, called "the charge transfer energy E_{ct}". Correspondingly, the total electron density change due to hydrogen bonding $\rho_H(1|1)$ is given as a sum of charges caused by the polarization, exchange, and "charge transfer" interactions. Classical electrostatic interaction corresponding to E_{es} has no effect on the change of electron distribution.

$$\rho_H(1|1) = \rho_4(1|1) - \rho_1(1|1) = \rho_{pl}(1|1) + \rho_{ex}(1|1) + \rho_{ct}(1|1) \tag{15}$$

$\rho_{ct}(1|1)$ is thus calculated by the following formula:

$$\rho_{ct}(1|1) = -\rho_2(1|1) - \rho_3(1|1) + \rho_1(1|1) + \rho_4(1|1) \tag{16}$$

By the use of these difference densities, ρ_{ex}, ρ_{pl}, ρ_{ct}, and ρ_H, we can also calculate individual components, μ_{ex}, μ_{pl}, μ_{ct}, and μ_H, of changes of dipole moment upon dimerization.

$$\mu_{ex} = \int \rho_{ex}(1|1)\mathbf{r}_1 d\tau_1 \tag{17}$$

$$\mu_{pl} = \int \rho_{pl}(1|1)\mathbf{r}_1 d\tau_1 \tag{18}$$

$$\mu_{ct} = \int \rho_{ct}(1|1)\mathbf{r}_1 d\tau_1 \tag{19}$$

$$\mu_H = \mu_{ex} + \mu_{pl} + \mu_{ct} = \mu_{dimer} - \mu_{monomers} \tag{20}$$

In the present paper, an analysis will be carried out for ρ_{pl}, ρ_{ex}, and ρ_{ct} and the results will be compared with the energy component and dipole moment analyses.

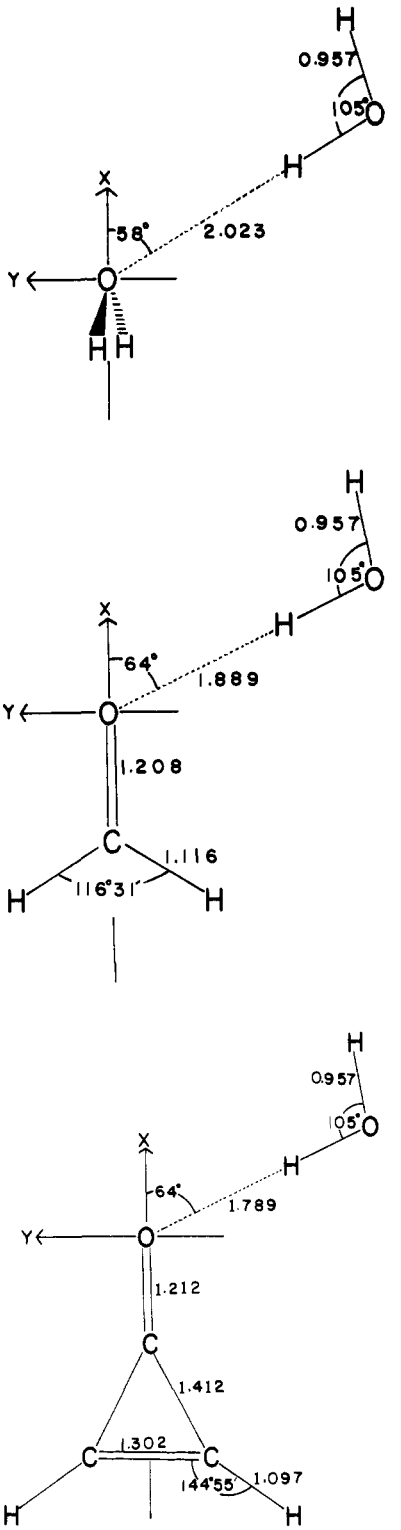

Figure 1. Geometries used for electron density analyses of water dimer, formaldehyde-water, and cyclopropenone-water systems. The numbers without units are in Å.

III. Basis Sets and Geometries

In the present analysis of ab initio SCF electron distribution and energy of H bonded systems, the 4-31G basis set with standard parametrization[6] is adopted, unless otherwise mentioned. The GAUSSIAN 70 program[7] is used for MO calculations, and a plotter program ZPLOT is used for electron density plots. Although the basis set dependency of H bond properties is recognized, their gross characteristics were found to be rather insensitive to the choice of basis

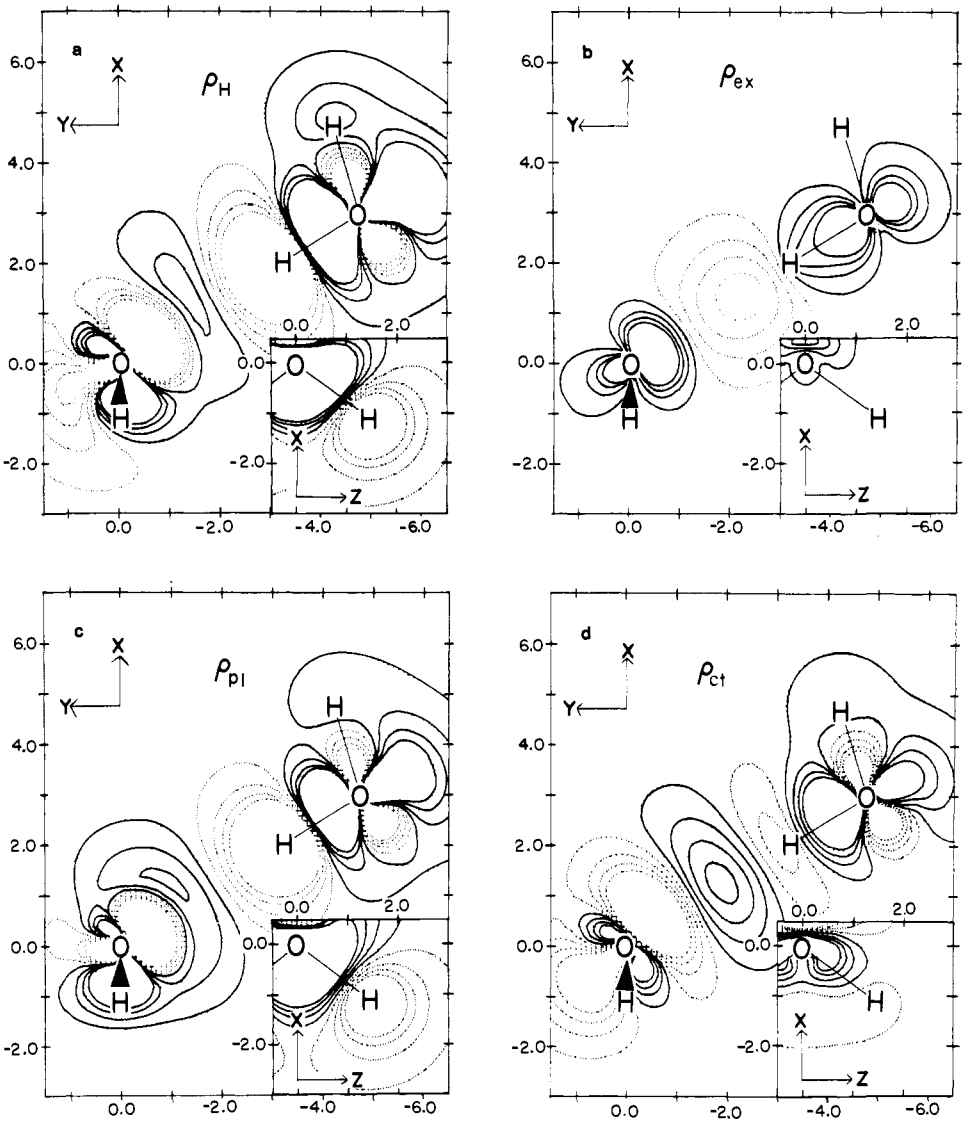

Figure 2. The electron density change and its components in the water dimer. Full lines indicate density increases and dotted lines indicate decreases. Values of these lines are successively ±0.2, ±0.6, ±1.0, and ±1.4 × 10^{-3} (Bohr^{-3}). The coordinates are in Bohr, relative to the oxygen atom of the proton acceptor.

set.[4] Therefore, the basis set dependency will not be examined in the present paper.

The monomer geometries in H bond systems are frozen to those of the isolated species, which is a required condition for the proposed analysis. They are taken from experimental results (the water molecule,[8] formaldehyde,[9] and cyclopropenone[10]). The adopted geometries of H bonded systems are shown in Figure 1. The structure of $(H_2O)_2$ is from a recent experiment[11] and H_2CO-H_2O from a previous calculation.[3] Since the most stable orientation of H_2O toward cyclopropenone is not known, a geometry optimization is carried out with the STO-3G basis set with standard parametrization.[12] Linear hydrogen bonding with a coplanar geometry, as shown in Figure 1, is found to be most stable, as will be discussed in section VI.

It is noteworthy that this system has the same orientation of water toward the C=O group as that in H_2C=O···H_2O, i.e., the angle between the O···H H bond line and the C=O is 64° with H_2O in the R_2CO molecular plane. This indicates that the H bond direction is not influenced by the inclusion of the cross-conjugated C=C double bond. The relationship between the double-bond conjugation and the H bond ability will be discussed later in section VI.

IV. Water Dimer

In Figure 2 the total electron density change $\rho_H(1|1)$ and its various components are plotted for $(H_2O)_2$ at the experimental geometry. The plot is made for the xy plane, which contains the proton-donor H_2O molecule and the proton-accepting oxygen atom of H_2O (Figure 1). In this figure, we also give as inserts densities on the xz plane including proton-acceptor water. The xy-plane maps are convenient for comparison between $(H_2O)_2$ and the H_2O-carbonyl compound systems to be discussed later, because of the close resemblance of geometries when looked upon from this angle, as was pointed out previously.[3] The corresponding total hydrogen bond energy and its components are given in the second column of Table I.

Although the total density change $\rho_H(1|1)$ in Figure 2 shows clearly the global feature of the electron redistribution due to the H bond formation, it is not easy to grasp mechanisms of the electron rearrangement. The analysis of partitioned density changes (ρ_{ex}, ρ_{pl}, and ρ_{ct}) will enable one to pinpoint the location and components of major changes.

The density change $\rho_{ex}(1|1)$ due to the exchange interaction in Figure 2 shows a large decrease (a negative value) in

Table I. The Hydrogen Bond Energy and Its Components from SCF Calculation with the 4-31G Basis Set[a]

System	Water dimer	Formaldehyde–water	Cyclopropenone–water	
O···H dist, Å	2.023	1.889	1.789	1.789[b]
E_{es}	8.98	9.49	13.50	10.98
E_{ex}	−4.19	−6.95	−10.48	−12.76
E_{pl}	0.47	0.77	1.27	1.23
E_{ct}	2.45	2.78	3.76	3.73
E_H	7.72	6.09	8.05	3.18

[a] For geometries shown in Figure 1. Energies are in kcal/mol, with a plus for the stabilization and a minus for destabilization. [b] For the approach of the H–O bond of water to the carbonyl oxygen, perpendicularly to the cyclopropenone plane.

Table II. Dipole Moment and Various Contributions to It for Water Dimer in Debye units (4-31G Basis Set)

	Absolute value	Components[a]		Expt[b]
		x	y	
$\mu_{monomers}$[c]	2.964	1.689	−2.435	2.11
Changes				
μ_{ex}	0.028	0.015	−0.023	
μ_{pl}	0.262	0.202	−0.168	
μ_{ct}	0.256	0.146	−0.211	
Sum μ_H	0.541	0.363	−0.402	(0.44)
μ_{dimer}	3.501	2.052	−2.837	2.601

[a] The coordinate system is that of Figure 1a. The dipole moment vector is directed from the positive charge to the negative charge. The z component is zero. [b] Reference 11. [c] The vector sum of monomer dipoles.

the O···H intermolecular region and a large increase in the intramolecular regions. It is also noted that such an electron redistribution takes place along the O···H–O H bond axis and its extension. In other words, little of the exchange effect is transmitted to the terminal hydrogen atoms of the proton donor or acceptor H_2O molecule. Dreyfus and Pullman pointed out this locality of the exchange effect in the linear formamide dimer.[13a]

Using MO's of isolated molecules, $\{A_i^0\}$ and $\{B_k^0\}$, and the overlap integral between them:

$$S_{ik} = \int A_i^0(1)B_k^0(1)\mathrm{d}v_1 \tag{21}$$

one can express ρ_{ex} to the second order of the overlap as follows:[14]

$$\rho_{ex}(1|1) = \{-4\sum_{i}^{occ}\sum_{k}^{occ} A_i^0(1)B_k^0(1)S_{ik} + 2\sum_{i}^{occ}\sum_{j}^{occ}\sum_{k}^{occ} A_i^0(1)A_j^0(1)S_{ik}S_{jk} + 2\sum_{i}^{occ}\sum_{k}^{occ}\sum_{l}^{occ} B_k^0(1)B_l^0(1)S_{ik}S_{il}\}/(1 - 2\sum_{i}^{occ}\sum_{k}^{occ} S_{ik}^2) \tag{22}$$

The first term in the bracket is the origin of the decrease in the interacting region; it is negative and has a large magnitude when A_i^0 and B_k^0 overlap substantially at the intermolecular region. The second and third terms are the main contributers to the density build-up in the molecules A and B, respectively. Since all the terms involve the overlap integral between MO's of A and B and the overlap is large only between MO's which are symmetric with respect to the O···H–O axis, the density change takes place mainly along the axis. It is also noted that the density decrease in the intermolecular region occurs in the neighborhood of the proton rather than the midpoint of O and H. This is due to the small size of the proton 1s orbital, which makes the overlap density $A_i^0(1)B_k^0(1)$ largest near the proton.

The density change $\rho_{pl}(1|1)$ due to the polarization effect is very large, as is seen in Figure 2. This is rather surprising in reference to a small polarization energy (0.47 kcal/mol) in Table I. One might interpret the small polarization energy as the differences between the stabilization due to the interaction between the density change and the other molecule's field and the intramolecular destabilization resulting from the deviation of the SCF electron density of the isolated molecule. As expected, in the proton-donor molecule, the transfer of the electron density from the H bonding H to the rest of the molecule is observed. For the proton-acceptor molecule, a density builds up in the interaction region to the upper left of the O···H axis, which is reasonable when one considers the direction of the dipole moment of the proton-donor molecule. One also recognizes the remarkable density decrease on the protons of the proton-acceptor molecule on the xz plane.

The electron density change $\rho_{ct}(1|1)$ due to the charge transfer or delocalization interaction, as shown in Figure 2, clearly demonstrates the charge migration from the proton acceptor to the proton donor. The rearrangement within the proton donor is caused appreciably by the coupling effect corresponding to E_{cp} in eq 14.[5] This trend was noticed by a gross population analysis in the earliest study of $(H_2O)_2$ and used to discuss the inadequacy of the localized model consisting only of the fictitious O–H···O fragment.[1] One can also notice the tremendous accumulation of bonding density in the O···H intermolecular region which flows from the oxygen lone-pair orbital of the proton acceptor. This positive bonding density is the origin of the covalent attractive force.

Now one can reexamine the total density difference map $\rho_H(1|1)$ of Figure 1 as the sum of the above three density changes. The following conclusions can be drawn.[13c]

(1) The large electron density loss on the H bonding proton and in the O···H region comes from two sources: the polarization effect which is most important on and around the proton and the exchange repulsion effect for the O···H intermolecular region.

(2) The increase of the density around the midpoint of the O···H is mainly due to the delocalization of electrons for a covalent formation, aided a little by the polarization of the proton acceptor.

(3) The increase in the density in the nonbonding OH of the proton donor is caused by both the charge transfer and polarization effects.

(4) The depletion of the density on the protons of the proton acceptor is due to the polarization.

In order to further examine roles of these different electronic contributions, the dipole moment of dimer and various contributions to its change (eq 17–20) are calculated. The results are shown in Table II.

The change due to the exchange effect μ_{ex} is found to be very small. This reflects the above mentioned local effect of exchange along the H bond line and the cancellation of the dipole changes along this line. On the other hand, the change due to polarization μ_{pl} is large, as is expected from a large ρ_{pl}. It is noted that the direction of μ_{pl} is substantially deviated from the H bond line (where μ^x/μ^y should be −0.625). This is because, while ρ_{pl} of the proton donor is important along the H bond line, ρ_{pl} of the proton acceptor is concentrated along the x axis, as can be seen in the xz-plane map, making μ_{pl}^x large. The change due to charge transfer μ_{ct} is as large as μ_{pl}. Since the charge transfer effect carries the charge mainly along the H bond line (Figure 2d), the direction of μ_{ct} is more or less parallel to it.

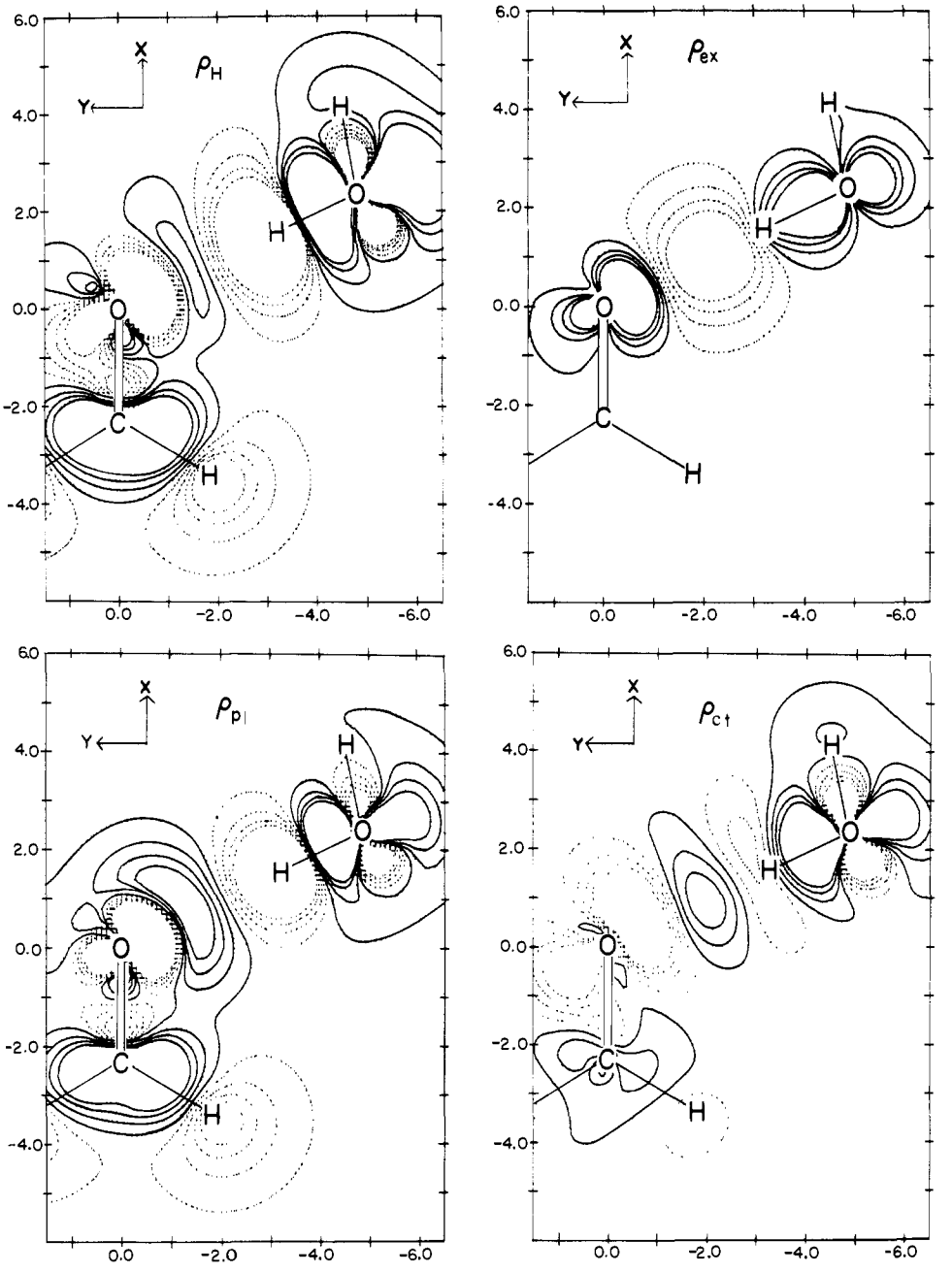

Figure 3. The electron density change and its components in the formaldehyde-water system. See Figure 2 for details.

Though the 4-31G basis set tends to overestimate the dipole moment compared to experiment[6,22] as is seen in Table II, the magnitude (0.541 D) of dipole enhancement due to dimerization is in reasonable agreement with the experimental estimate (0.44 D).[11]

V. Formaldehyde-Water Complex

The same analysis of the electron density changes and the energy components is carried out for the $H_2CO\cdots H_2O$ H bonded complex for the equilibrium geometry of Figure 1. The results are shown in Table I and Figure 3. The comparison of Figures 2 and 3 reveals a great similarity and some specific differences between $(H_2O)_2$ and the present system.

The striking similarity is found for $\rho_{ex}(1|1)$; the maps for $(H_2O)_2$ and $H_2CO\cdots H_2O$ are virtually indistinguishable. This is because of the short-range nature of the exchange interaction and because the existence of the carbonyl π orbitals has only a minor effect on the exchange interaction due to their orthogonality to O···H-O σ orbitals (see eq 22). In $\rho_{pl}(1|1)$, in addition to the similarity in the part of the proton-donor H_2O molecule, the characteristic role of the polarization effect is noted in the formaldehyde part. A considerable amount of electron density is moved from the hydrogen atoms to the carbonyl carbon atom. Also, a substantial charge redistribution from the $2p\pi$ AO of the carbon atom to that of the oxygen atom takes place, though this is not seen in Figure 2 because mapping is for the xy plane, the nodal plane of the π orbitals. This general trend of the electron move, from H to C, from C to O and the polarization toward the proton donor within O, is qualitatively parallel to the direction of the molecular dipole moment of the proton donor H_2O. Thus the polarization effect is the predominant factor for the intramolecular charge redistribution.

The charge transfer contribution, $\rho_{ct}(1|1)$, exhibits in the O···H-O intermolecular region similar trends as that for $(H_2O)_2$, i.e., a substantial electron density transfer to H_2O, an accumulation of bonding density around the midpoint of

O···H, and the loss of density from the H bonding proton. The charge transfer interaction, jointly with the polarization interaction, also plays a role in weakening the carbonyl C=O bond. The decrease of C=O bonding density by charge transfer is caused by σ MO's. The third highest MO of H_2CO which has a substantial C=O bonding character contributes appreciably, together with the highest σ MO, to the charge transfer interaction. The decrease of electron density from this MO due to charge transfer results in weakening of the C=O bond. As a whole, however, the charge transfer interaction does not cause as much intramolecular electron density rearrangement as the polarization interaction does.

VI. Cyclopropenone-Water Complex

As the last example of the density analysis, the cyclopropenone-water H bond system will be studied. Motivation for this study is twofold. Hydrogen bonding to cyclopropenone has been of special experimental interest.[15,16] From the electronic point of view, the effect of the C=C double bond to the properties of the carbonyl group and consequently to the H bond strength and geometry will provide an insight for better understanding of the H bond. Since the C=O bond lengths for formaldehyde and cyclopropenone are almost the same, this comparison is rather tempting.

Before proceeding to the H bond system, electronic structures of cyclopropenone itself should be examined. Cyclopropenone and its derivatives are known to have unusual stabilities for their strained structures.[17] Cyclopropenone's unique stability is explained qualitatively in terms of the contribution of the dipolar resonance structure. The large experimental value of the dipole moment (4.39 D)[10] has been ascribed to a large π electron polarization. In addition, the low-energy carbonyl ir absorption suggests a high degree of single-bond character in the C=O bond,[17] implicating the importance of the dipolar structure. A few semiempirical[18,19] and ab initio[20,21] calculations have been carried out for this molecule. Clark and Lilley's ab initio study[20] reported the gross population, the dipole moment, and some localization energies with a small basis set. Harshbarger, Kuebler, and Robin present the electronic impact and photoelectron spectra of the molecule and assign the ionization potentials with the aid of SCF calculations of double ζ quantity.[21]

In Figure 4, we present briefly the result of the 4-31G basis MO calculation for cyclopropenone and formaldehyde. A comparison of atomic populations indicates that the carbonyl π electrons are more polarized in cyclopropenone than in formaldehyde, as can be interpreted in terms of contribution of resonance structures as follows:

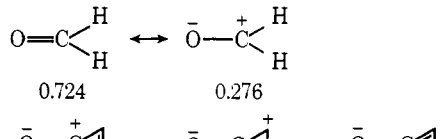

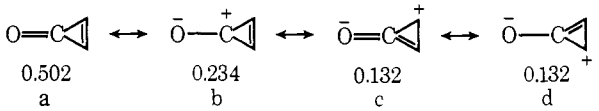

The importance of the dipole resonance structures (b, c, and d) in cyclopropenone can be correlated with experiments. The smaller contribution of the double bond structure is related to the low energy of the CO stretching. The large polarization is also reflected in the large calculated dipole moment (5.08 D), though the 4-31 basis set tends to overestimate the polarization and, as the consequence, the dipole moment. The terminal hydrogen atoms in cyclopropenone are more positively charged than in formaldehyde.

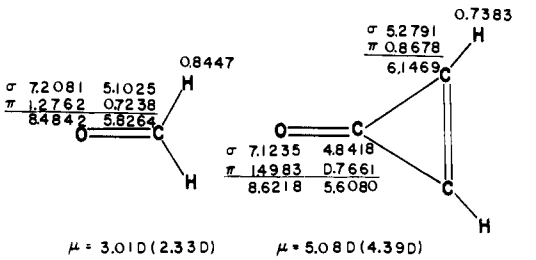

Figure 4. Gross atomic populations and dipole moments by a 4-31G basis set. The dipole moments in parentheses are experimental values: H_2O, A. L. McClellan, "Tables of Experimental Dipole Moments", W. H. Freeman, San Francisco, Calif., 1963; and cyclopropenone, ref 10.

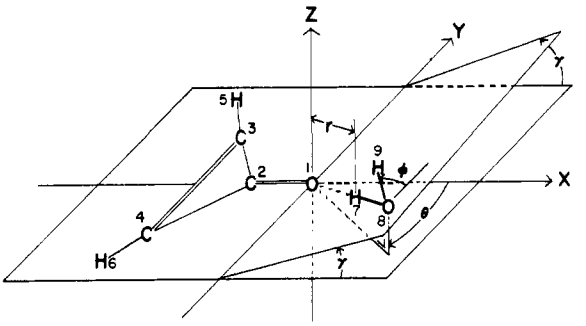

Figure 5. The general conformation of the cyclopropenone-H_2O system defined by r, θ, γ, and ϕ.

Taking into account these unique features of cyclopropenone, we now determine the most stable geometry of the cyclopropenone-water H bonded system. Figure 5 defines the general conformation of the H bonded system and adopted variables; r, the O···H distance; θ, the angle between the C=O axis (x axis) and the O···HO straight line; γ, the angle of rotation of the O···O y plane around the y axis; and ϕ, the rotation angle of the non-H bonding proton H_9 from the O···O y plane. Previous calculations indicate that, although at the equilibrium geometry the electrostatic energy E_{es}, the exchange energy E_{ex}, and the charge-transfer energy E_{ct} are all important, the relative direction of approach of the two molecules is often determined by the electrostatic energy.[3,22] For an approach of a small polar molecule such as a water molecule, the electrostatic potential due to the electron distribution and nuclei of the polar partner molecule qualitatively predicts the direction of approach.[23,24] This would be particularly true for cyclopropenone which is extremely polar. The electrostatic potential map (not shown) for cyclopropenone suggests that $\theta \sim 60°$, $\gamma \sim 0°$, and $\phi \sim 0°$ is the most probable direction of approach. An actual angular optimization run was carried out with MO calculations with the STO-3G basis set for a fixed $r = 1.89$ Å, an optimum for H_2CO-H_2O with a minimal STO set.[3] After 23 different calculations and fourth-order polynomial fits, the most favorable direction of approach is determined to be $\theta = 63.5°$, $\gamma = 0°$, and $\phi = 0°$. These values are very close to the optimized angles ($\theta = 63.9°$, $\gamma = 0°$, and $\phi = 0°$) for the H_2CO···H_2O system calculated with a minimal STO basis set,[3] supporting the proposition that H bonding occurs in the direction of the hybridized lone-pair orbital (in this case 60° for sp^2 hybridization[3]). Neglecting the very slight difference of the angle θ, we assume that both H bonded systems have common optimized angles, $\theta = 64°$, $\gamma = 0°$, and $\phi = 0°$, for the sake of comparison. Next the O···H distance (r) was changed for the fixed angles above. Eight MO calculations and a fourth-order polynomial fit, for this system and H_2CO-H_2O with a common STO-3G basis set, give the potential energy curves shown in Figure

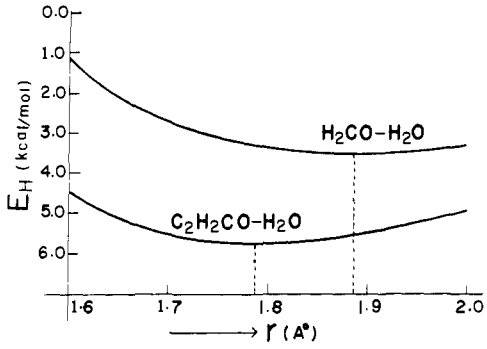

Figure 6. The potential energy curve as a function of the O···H distance for the formaldehyde-water and cyclopropenone-water systems with the STO-3G basis set.

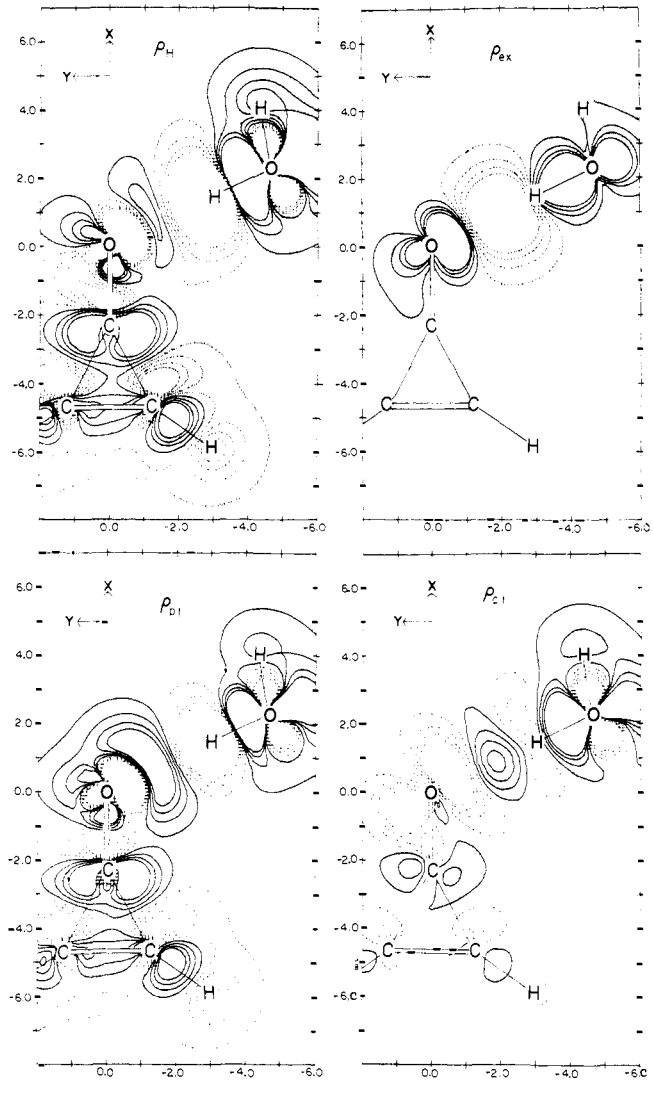

Figure 7. The electron density change and its components in the cyclopropenone-water system. See Figure 2 for details.

6. It is noted in Figure 6 that the cyclopropenone-water system has a shorter O···H distance (~1.789 Å) than the formaldehyde-water system (~1.889 Å). Accordingly, the former has a stronger H bond ($E_H \sim 5.75$ kcal/mol) than the latter ($E_H \sim 3.50$ kcal/mol). In order to assess the origin of the stabilization, the energy decomposition analysis is carried out, as shown in Table I, with the 4-31G basis set at the STO-3G optimized minimum for cyclopropenone-water.[25] The columns 3 and 4 of Table I indicate that the larger stabilization of the cyclopropenone-water system is mainly

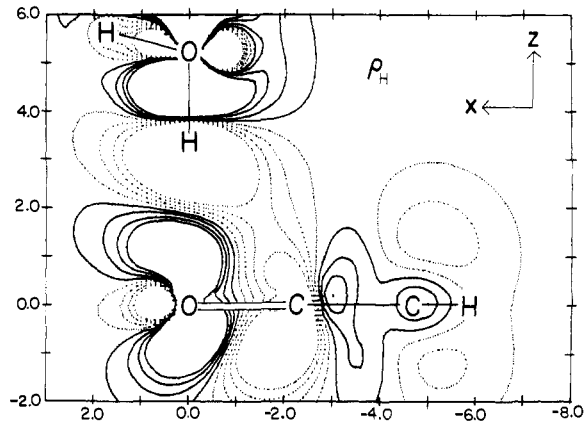

Figure 8. The total electron density change for the π-type interaction in the cyclopropenone-water system. See Figure 2 for details.

due to the electrostatic energy E_{es}, as was expected from the population analysis and the dipole moment of cyclopropenone and formaldehyde. The smaller O···H distance in cyclopropenone-H_2O brings about a larger contribution of E_{ex} and E_{ct} as well.

The electron density changes for the present system for the geometry given in Figure 1 are shown in Figure 7. The features commonly observed in $(H_2O)_2$ and H_2CO-H_2O as well as in this system will not be discussed again. But some unique features of this system will be examined. The exchange contribution $\rho_{ex}(1|1)$ shows a very large decrease of density in the intermolecular region, reflecting a larger E_{ex} than in the H_2CO-H_2O system. The polarization contribution $\rho_{pl}(1|1)$ shows that the water molecule becomes more polarized here than in the H_2CO-H_2O system due to the larger polarity of the proton acceptor molecule. As for cyclopropenone, the polarization occurs mainly within each bond, resulting in the charge alternation which may be represented as follows:

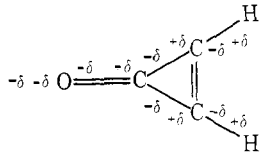

The charge transfer contribution $\rho_{ct}(1|1)$ here is larger than in H_2CO-H_2O due to the smaller distance in the present case, but is qualitatively very similar and has only a minor effect for the charge redistribution in the ring part of cyclopropenone. This small effect of the charge transfer interaction to the charge redistribution within a molecule seems to be characteristic of weak interactions such as H bonding, whereas in chemical reactions the charge transfer plays an extremely important role.[26] The effect of polarization on the total density change $\rho_H(1|1)$ is more profound in the present system than the other systems studied in the paper.

π-Type H bonding, in which the proton donor approaches the π electron cloud of the proton acceptor, is recognized in some cases.[27] Our previous study on H_2CO-H_2O indicates that π-hydrogen bonding suffers from a larger exchange repulsion and a smaller charge transfer stabilization though the electrostatic stabilization is comparable to normal H bonding.[3] Since cyclopropenone is more polar than formaldehyde, the electrostatic stabilization may make π H bonding more stable. Ab initio optimization of the O···H distance was carried out first at the STO-3G SCF level for an approach of the water OH bond above the oxygen atom and perpendicular to the cyclopropenone molecular plane, with the non-H bonding proton of H_2O trans to the carbonyl

bond.[3] The most stable O···H distance is 2.08 Å with a stabilization energy of 2.36 kcal/mol. This is, as expected, larger than 0.40 kcal/mol at 2.5 Å for H_2CO–H_2O with a minimal STO basis set.[3] The energy decomposition and electron distribution analyses were carried at the same O···H distance (1.789 Å) and with the same basis set (4-31G) as in the normal H bonding case in order to facilitate the comparison. The results in the last column of Table I compared with column 4 indicate that π bonding has a smaller electrostatic stabilization and a larger exchange repulsion, whereas the polarization and charge transfer contributions are unchanged. The large exchange repulsion is visualized in Figure 8 as a larger area of the negative charge accumulation than in the normal case (ρ_H of Figure 7).

VII. Conclusions

We have analyzed the changes in the electron distribution due to hydrogen bonding. The partitioning scheme, similar to that used for the energy decomposition analysis of the hydrogen bond energy, was applied to three hydrogen bonding systems. From the results one can draw the following common conclusions.

(1) The exchange interaction gives rise to the antibonding density in the intermolecular region, corresponding to the negative value (repulsion) of the exchange interaction energy. The compensating positive density is accumulated locally on the three atoms X–H···Y which directly participate in H bonding. The exchange interaction does not cause any density change in the other parts of the molecules. This effect is also related to the minor change of the dipole moment (μ_{ex}).

(2) Polarization causes the most significant charge redistribution among the three contributions, in spite of the smallest contribution to the energy among four terms. In the proton-donor water molecule, the H bonded proton loses a substantial amount of the electron density to the oxygen orbitals along the O–H···O line. In the proton-acceptor molecule the charge redistribution is attributable almost solely to the polarization interaction. This effect causes the polarization of each lone pair and bond, resulting in the charge alternation throughout the acceptor molecule. Such an important role of the polarization is reflected in the large change of the dipole moment (μ_{pl}). Its direction does not coincide with the O···HO axis because of the large polarization of terminal protons.

(3) The charge transfer interaction carries the charge from the proton acceptor to the proton donor. The electron rearrangement is not local to the X–H···Y fragment, but reaches further ends of molecules. A positive bonding charge is accumulated near the midpoint of the H···Y intermolecular region, though its effect is largely canceled out by a large negative exchange density near the proton in the same region. The change of dipole moment by this interaction (μ_{ct}) occurred almost parallel to the direction of charge migration along the H bond line.

The exchange repulsion is the main cause of the unstability of π hydrogen bonding. This is noticed clearly in the accumulation of a large negative charge in the interaction region.

As is mentioned above, each interaction plays a characteristic role in the electron rearrangement. The electron distribution analysis used in the present paper sheds light on the identification of such roles by visualizing the changes and specifying regions of particular importance. In the present paper the analysis has been limited to the ground state of hydrogen bonded complexes. The application of the method to excited states and other types of molecular complexes such as electron donor–acceptor complexes is straightforward and would be very useful for understanding the nature of such bonding.

Acknowledgment. The authors are grateful to Dr. W. A. Lathan for many helpful discussions, comments, and programming advice. The research is in part supported by the National Science Foundation (Grant GP-43406X) and the Center for Naval Analyses of the University of Rochester.

References and Notes

(1) K. Morokuma and L. Pedersen, *J. Chem. Phys.*, **48**, 3275 (1968).
(2) P. A. Kollman and L. C. Allen, *Chem. Rev.*, **72**, 283 (1972).
(3) K. Morokuma, *J. Chem. Phys.*, **55**, 1236 (1971).
(4) S. Iwata and K. Morokuma, *J. Am. Chem. Soc.*, **95**, 7563 (1973).
(5) Recently a method to define E_{ct} independently and more clearly has been defined: K. Kitaura and K. Morokuma, to be published.
(6) The exponents and scale factors are those in R. Ditchfield, W. J. Hehre, and J. A. Pople, *J. Chem. Phys.*, **54**, 724 (1971).
(7) W. J. Hehre, W. A. Lathan, R. Ditchfield, M. D. Newton, and J. A. Pople, Program No. 236 Quantum Chemistry Program Exchange, Indiana University, 1973.
(8) K. Kuchitsu and L. S. Bartell, *J. Chem. Phys.*, **36**, 2460 (1962).
(9) K. Takagi and T. Oka, *J. Phys. Soc. Jpn.*, **18**, 1174 (1963).
(10) R. C. Benson, W. H. Flygare, M. Oda, and R. Breslow, *J. Am. Chem. Soc.*, **95**, 2772 (1973).
(11) T. R. Dyke and J. S. Muenter, *J. Chem. Phys.*, **60**, 2929 (1974).
(12) The exponents and scale factors are those in W. J. Hehre, R. F. Stewart, and J. A. Pople, *J. Chem. Phys.*, **51**, 2657 (1969).
(13) (a) M. Dreyfus and A. Pullman, *Theor. Chim. Acta*, **19**, 20 (1970); (b) P. A. Kollman and L. C. Allen, *J. Chem. Phys.*, **52**, 5085 (1970). (c) The ρ_H plots of the present work may look a little different from plots in ref 13a and 13b. For instance, ρ_H has a positive area in the interaction region in this paper, whereas ref 13a and 13b show none. This is mainly due to the difference of geometry. Here the optimal geometry puts the hybridized lone pair of the oxygen atom to the direction of the O···H–O bond, while in ref 13a and 13b, the lone pair is not toward the O···H–O line along which the plot is shown.
(14) H. Fujimoto, S. Yamabe, and K. Fukui, *Bull. Chem. Soc. Jpn.*, **44**, 2936 (1971).
(15) R. Breslow and G. Ryan, *J. Am. Chem. Soc.*, **89**, 3073 (1967).
(16) The monohydrate structure of diphenylcyclopropenone was confirmed by the ir spectra: F. Toda and K. Akagi, *Tetrahedron Lett.*, 3735 (1968).
(17) K. T. Potts and J. S. Baum, *Chem. Rev.*, **74**, 189 (1974).
(18) A. Watanabe, H. Yamaguchi, Y. Amako, and H. Azumi, *Bull Chem. Soc. Jpn.*, **41**, 2196 (1968).
(19) D. J. Bertelli and T. G. Andrews, Jr., *J. Am. Chem. Soc.*, **91**, 5280 (1969).
(20) D. T. Clark and D. M. J. Lilley, *Chem. Commun.*, 147 (1970).
(21) W. R. Harshbarger, N. A. Kuebler, and M. B. Robin, *J. Chem. Phys.*, **60**, 345 (1974).
(22) K. Morokuma, S. Iwata, and W. A. Lathan, "The World of Quantum Chemistry", R. Daudel and B. Pullman, Ed., D. Reidel Publishing Co., Dordrecht, Holland, 1974, pp 277–316.
(23) R. Bonaccorsi, C. Petrongolo, E. Scrocco, and J. Tomasi, *Theor. Chim. Acta*, **20**, 331 (1971).
(24) W. A. Lathan and K. Morokuma, *J. Am. Chem. Soc.*, **97**, 3615 (1975).
(25) Usually the 4-31G set gives a larger O···H distance than the STO-3G set. For instance, the optimized O···H distance of the formaldehyde–water system is calculated to be 2.019 Å with the 4-31 set, which is 0.13 Å longer than that (1.889 Å) by the STO-3G basis set. Therefore, the 4-31G set is expected to have the slightly longer (~0.1 Å) optimized distance than that given in Figure 1c as to cyclopropenone–water system. Although the full 4-31G optimization was not carried out at this time, the essential part of our discussion should be unaffected.
(26) K. Fukui and H. Fujimoto, *Bull. Chem. Soc. Jpn.*, **42**, 3399 (1969).
(27) G. C. Pimentel and A. L. McClellan, "The Hydrogen Bond", W. H. Freeman, San Francisco, Calif., 1960.